Fiber Connection Pattern-Guided Structured Sparse Representation of Whole-Brain fMRI Signals for Functional Network Inference

Xi Jiang[1], Tuo Zhang[2,1], Qinghua Zhao[3], Jianfeng Lu[3], Lei Guo[2], and Tianming Liu[1]

[1] Cortical Architecture Imaging and Discovery Laboratory, Department of Computer Science and Bioimaging Research Center, The University of Georgia, Athens, GA, USA
superjx2318@gmail.com
[2] School of Automation, Northwestern Polytechnical University, Xi'an, P. R. China
[3] School of Computer Science and Engineering,
Nanjing University of Science and Technology, Nanjing, P. R. China

Abstract. A variety of studies in the brain mapping field have reported that the dictionary learning and sparse representation framework is efficient and effective in reconstructing concurrent functional brain networks based on the functional magnetic resonance imaging (fMRI) signals. However, previous approaches are pure data-driven and do not integrate brain science domain knowledge when reconstructing functional networks. The group-wise correspondence of the reconstructed functional networks across individual subjects is thus not well guaranteed. Moreover, the fiber connection pattern consistency of those functional networks across subjects is largely unknown. To tackle these challenges, in this paper, we propose a novel fiber connection pattern-guided structured sparse representation of whole-brain resting state fMRI (rsfMRI) signals to infer functional networks. In particular, the fiber connection patterns derived from diffusion tensor imaging (DTI) data are adopted as the connectional features to perform consistent cortical parcellation across subjects. Those consistent parcellated regions with similar fiber connection patterns are then employed as the group structured constraint to guide group-wise multi-task sparse representation of whole-brain rsfMRI signals to reconstruct functional networks. Using the recently publicly released high quality Human Connectome Project (HCP) rsfMRI and DTI data, our experimental results demonstrate that the identified functional networks via the proposed approach have both reasonable spatial pattern correspondence and fiber connection pattern consistency across individual subjects.

Keywords: Structured sparse representation, functional network, fiber connection pattern, resting state functional MRI, diffusion tensor imaging.

1 Introduction

Sparse representation has received increasing interests in the brain mapping field for functional magnetic resonance imaging (fMRI) signal analysis and functional brain network inference based on the assumption that each brain fMRI signal can be

N. Navab et al. (Eds.): MICCAI 2015, Part I, LNCS 9349, pp. 133–141, 2015.
DOI: 10.1007/978-3-319-24553-9_17

represented as sparse linear combination of a set of signal basis [1-3]. Recent studies have widely reported that the dictionary learning and sparse representation framework is efficient and effective in reconstructing concurrent functional brain networks based on either task-based or resting state fMRI (rsfMRI) data [1-3]. One possible limitation of previous approaches, however, is that it is a pure data-driven regression procedure and does not integrate brain science domain knowledge when reconstructing functional networks. The group-wise correspondence of the functional networks across subjects is thus not well guaranteed. Moreover, the fiber connection pattern consistency of the reconstructed functional networks across subjects is largely unknown. In the neuroscience field, it is widely believed that the fiber connections are the substrates of brain functions [4].

To tackle the above-mentioned two challenges, in this paper, we propose a novel fiber connection pattern-guided structured sparse representation of whole-brain rsfMRI signals to infer functional networks. Note that previous efforts have been devoted to fiber connectivity-constrained conventional functional network (node and connectivity) analysis (e.g., [5]), while we focus on fiber connection pattern-constrained identification of functionally consistent brain regions, which are simply called 'functional network' in this paper. In particular, the fiber connection patterns derived from diffusion tensor imaging (DTI) data are adopted as the connectional features to perform group-wise consistent fine-granularity cortical parcellation across subjects based on our previous methods in [6]. Those consistent parcellated regions are then employed as the group structured constraint to guide group-wise multi-task sparse representation of whole-brain rsfMRI signals to reconstruct functional networks. Theoretically, structured multi-task sparse representation [7] defines a specific structure (e.g., groups, trees, or graphs) on the multi-tasks, and achieves both intra-group homogeneity and intra/inter-group sparsity via combined ℓ_1 and ℓ_2 -norms [7]. Our premise is that cortical vertices within the same parcellated cortical region which have similar fiber connection patterns should potentially play similar roles in brain function. Therefore, integrating those group-wise consistent parcellated regions across subjects as the group structured constraint can effectively handle the above-mentioned two challenges and improve the functional network reconstruction by constraining both intra-group homogeneity and intra/inter-group sparsity.

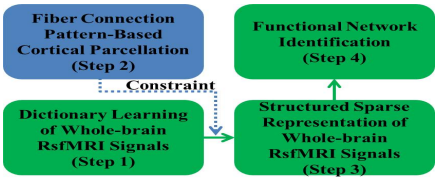

Fig. 1. The flowchart of our proposed framework.

2 Materials and Methods

2.1 Data Acquisition and Pre-processing

We used the high-quality rsfMRI [8] and DTI [9] data in the Human Connectome Project (HCP) (Q1 release) to develop and evaluate the proposed framework (Fig. 1).

Ten subjects were adopted as a test bed in this paper. The major acquisition parameters of rsfMRI data are 220mm/0.72s/33.1ms of FOV/TR/TE, 1200 time points, 90×104×72 dimension, and 2.0mm isotropic voxels. The pre-processing of rsfMRI data is referred to [8]. The major acquisition parameters of DTI data are 210×180/5520ms/89.5ms of FOV/TR/TE, 90 directions, 168×144 matrix, and 1.25mm isotropic voxels. Pre-processing of DTI data is referred to [6].

2.2 Dictionary Learning of Whole-Brain rsfMRI Signals

In our framework (Fig. 1), an over-complete dictionary $\mathbf{D} \in \mathbb{R}^{t \times k}$ (t is the signal time points and k is the dictionary atoms) was firstly learned from the whole-brain rsfMRI signals $\mathbf{X}=[\mathbf{x}_1, \mathbf{x}_2,\ldots,\mathbf{x}_n] \in \mathbb{R}^{t \times n}$ (n is the cortical vertices, $k>t$ and $k<<n$ [10]) of each subject using an effective online dictionary learning algorithm [10] assuming that the rsfMRI signals $\mathbf{X}$ can be represented as sparse linear combination of a set of signal basis (dictionary atoms) [10]. Specifically, for each subject, the whole-brain rsfMRI signals were extracted, normalized to zero mean and standard deviation of 1 [10], and aggregated into a matrix $\mathbf{X} \in \mathbb{R}^{t \times n}$. An empirical cost function considering the average loss of regression to n signal vectors was then defined in Eq. (1):

$$f_n(\mathbf{D}) \triangleq \frac{1}{n}\sum_{i=1}^{n} \ell(\mathbf{x}_i, \mathbf{D}) \tag{1}$$

$$\ell(\mathbf{x}_i, \mathbf{D}) \triangleq \min_{\boldsymbol{\alpha}_i \in \mathbb{R}^k} \frac{1}{2}||\mathbf{x}_i - \mathbf{D}\boldsymbol{\alpha}_i||_2^2 + \lambda||\boldsymbol{\alpha}_i||_1 \tag{2}$$

where the ℓ_1 regularization in Eq. (2) was adopted to generate a sparse resolution of $\boldsymbol{\alpha}_i$. $\mathbf{D}$ and $\boldsymbol{\alpha}$ were alternatively updated and learned [10]. The learned $\mathbf{D}$ was adopted as the regressors to perform conventional sparse representation and the proposed structured sparse representation of brain rsfMRI signals as detailed in Section 2.4.

2.3 Fiber Connection Pattern Based Cortical Parcellation for Constraint

We performed fiber connection pattern based cortical parcellation based on DTI data using our methods in [6]. Briefly, for each cortical vertex, we extracted the white matter fiber bundle consisting of fiber tracts emanating from the neighborhood (5 mm sphere) of the cortical vertex. The connection pattern of the extracted fiber bundle was then described as a 144 dimensional connectional descriptor using the trace-map model developed in [11]. Based on the fiber connectional descriptor of each cortical vertex, the cortical parcellation was performed to group-wisely and gradually parcellate cortical surfaces into consistent fine-granularity patches across subjects under a hierarchical scheme. The initial cluster centers and cluster numbers within each hierarchical level were determined via adaptive affinity propagation [6] based on the recently publicly released 358 cortical landmarks [11] which possess consistent white matter fiber connection patterns across subjects. Other cortical vertices were then classified into correspondent clusters based on the similarity of the connectional descriptors to achieve intra-level parcellation using the group-wise implementation of expectation maximization [6] under the spatial constraint of a group of subjects.

The same intra-level parcellation procedure was repeated in the next hierarchical level based on the parcellation results of the previous level. A group-wise hidden Markov random field smoothing approach [6] was also adopted to prevent the potential disconnected clusters. The resulted consistent parcellated cortical regions across subjects were employed as the group structured constraint to guide the sparse representation of rsfMRI signals as illustrated in Fig. 2 and detailed in Section 2.4.

2.4 Structured Sparse Representation of Whole-Brain rsfMRI Signals

The LASSO [12] has been widely used for sparse representation, and is defined as:

$$\hat{\boldsymbol{\alpha}} = argmin\ell(\boldsymbol{\alpha}) + \lambda\phi(\boldsymbol{\alpha}) \tag{3}$$

where $\ell(\boldsymbol{\alpha})$ is the empirical loss function, $\phi(\boldsymbol{\alpha})$ is the penalty term, and λ>0 is the regularization parameter. As illustrated in Fig. 2a, once we learned dictionary $\mathbf{D}\epsilon\mathbb{R}^{t\times k}$ (Section 2.2), the conventional LASSO to perform regression of rsfMRI signals $\mathbf{X}\epsilon\mathbb{R}^{t\times n}$ to obtain a sparse coefficient matrix $\boldsymbol{\alpha}\epsilon\mathbb{R}^{k\times n}$ was defined as:

$$\hat{\boldsymbol{\alpha}} = argmin \sum_{i=1}^{n} \frac{1}{2} ||\mathbf{x}_i - \mathbf{D}\boldsymbol{\alpha}_i||_2^2 + \lambda \sum_{i=1}^{n}\sum_{j=1}^{k} \left|\boldsymbol{\alpha}_i^j\right| \tag{4}$$

where $\ell(\boldsymbol{\alpha})$ is defined as the least square loss, and $\phi(\boldsymbol{\alpha})$ is the ℓ_1-norm regularization term to induce sparsity. $\boldsymbol{\alpha}_i^j$ is the coefficient element at the i-th column and j-th row. k and λ were experimentally determined (k=400 and λ=1.5). This conventional LASSO approach in Eq. (4) is pure data-driven.

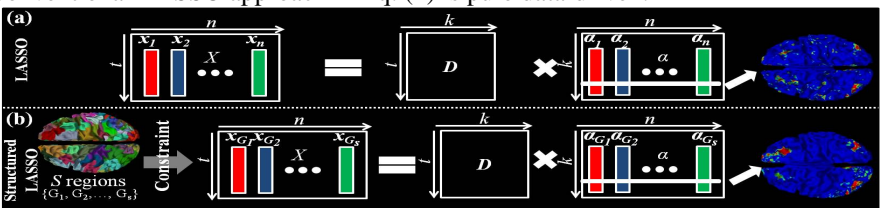

Fig. 2. The illustration of (a) conventional LASSO and (b) the proposed structured LASSO.

In this paper, we proposed a novel structured sparse representation (or structured LASSO) approach. As shown in Fig. 2b, the group-wise consistent parcellated cortical regions (Section 2.3) were adopted as the group structured constraint to guide LASSO. Based on the premise that vertices within the same parcellated cortical region which have similar fiber connection patterns should potentially play similar roles in brain function, the rsfMRI signals of those vertices should share similar regression weights for functional network reconstruction. We aimed to constrain both intra-group homogeneity and intra/inter-group sparsity for LASSO, and defined the structured LASSO as follows:

$$\hat{\boldsymbol{\alpha}} = argmin \sum_{i=1}^{n} \frac{1}{2} ||\mathbf{x}_i - \mathbf{D}\boldsymbol{\alpha}_i||_2^2 + \lambda \sum_{i=1}^{n}\sum_{j=1}^{k} \left|\boldsymbol{\alpha}_i^j\right| + (1-\lambda) \sum_{j=1}^{k}\sum_{s=1}^{S} \omega_s \left\|\boldsymbol{\alpha}_{G_s}^j\right\|_2 \tag{5}$$

where the rsfMRI signals $\mathbf{X}$ are categorized into S structured groups $\{G_1, G_2, \ldots, G_s\}$ $s = 1, \ldots, S$ based on the S parcellated cortical regions (Fig. 2b). ω_s is the weight

coefficient of $\left\|\boldsymbol{\alpha}_{G_s}^{j}\right\|_2$. The conventional LASSO adopted the ℓ_1-norm regularization term to induce sparsity (Eq. (4)), while our proposed structured LASSO introduced a ℓ_2-norm penalty term to improve the intra-group homogeneity, and also kept the ℓ_1-norm penalty to induce both intra- and inter-group sparsity (Eq. (5)). The detailed parameter selection and solution of Eq. (5) was referred to [7]. We adopted the public SLEP software package (http://www.public.asu.edu/~jye02/Software/SLEP/) to solve the problem and to obtain $\boldsymbol{\alpha}\epsilon\mathbb{R}^{k\times n}$. The values of two major parameters k and λ were experimentally determined using cross-validation (k=400 and λ=0.15). From brain science perspective, each learned dictionary can be viewed as the temporal pattern of a functional network, and each row of learned $\boldsymbol{\alpha}$ (non-zeros coefficients) were mapped back to cortical surface (Figs. 2a-2b) to obtain the cortical spatial maps of the network. To identify and quantitatively characterize the meaningful functional networks, we adopted the functional networks templates provided in [13]. The specific row of $\boldsymbol{\alpha}$ with the most spatial pattern similarity (defined as Jaccard similarity coefficient [14] $\mathrm{J}(\mathrm{A},\mathrm{T}) = |\mathrm{A}\cap\mathrm{T}|/|\mathrm{A}\cup\mathrm{T}|$, A and T are spatial maps of a specific row of $\boldsymbol{\alpha}$ and a template, respectively) with a specific network template was identified as the corresponding functional network. More details are in [3].

3 Experimental Results

3.1 Comparison of Identified Functional Networks

We compared the identified functional networks via the structured LASSO and conventional LASSO. The widely known 'default mode network' (DMN) [13] was adopted as the example here for demonstration. First, Fig. 3 shows that the spatial patterns of DMN via the structured LASSO (Fig. 3a) have better group-wise correspondence and higher similarity with the DMN template [13] across subjects compared with those via the conventional LASSO (Fig. 3b). Quantitatively, the mean spatial similarity of identified DMNs for each individual subject is 0.31±0.03 via the structured LASSO, which is larger than the conventional LASSO (0.18±0.01). The spatial similarity of group-averaged DMN with the structured LASSO (0.53) is also improved compared with the conventional LASSO.

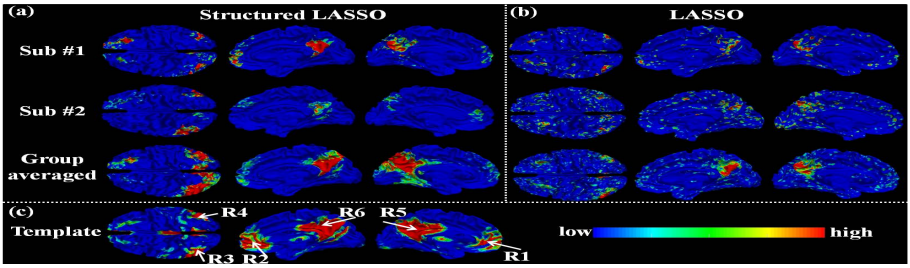

Fig. 3. Spatial patterns of identified DMN via (a) the proposed structured LASSO and (b) conventional LASSO of two example subjects and across all ten subjects. (c) shows the spatial pattern of the DMN template. The six major regions of DMN are labeled as R1 to R6, respectively. The color bar of the spatial patterns is shown in (c).

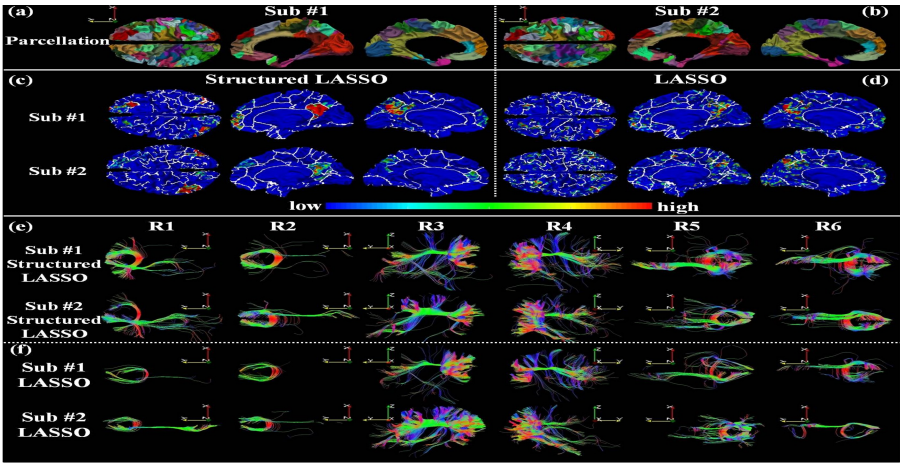

Fig. 4. (a)-(b): Parcellated cortical regions of the two example subjects. The corresponding regions are labeled by the same color. (c)-(d): Co-visualization of the cortical parcellation (white curves delineate the boundaries of regions) and spatial pattern of DMN via the (c) structured LASSO and (d) conventional LASSO of the two subjects. (e)-(f): DTI-derived white matter fiber bundles connecting to the six regions of DMN (R1 to R6 in Fig. 3c) via the (e) structured LASSO and (f) conventional LASSO of the two subjects.

Second, Figs. 4a-4b show that the parcellated cortical regions (65 in total) of the two example subjects have reasonable correspondence as reference. The co-visualization of the cortical parcellation and the spatial pattern of DMN in Figs. 4c-4d shows that all six major regions of DMN (Fig. 3c) have reasonable coincidence with specific parcellated regions via the structured LASSO (Fig. 4c), as expected, while are not well matched with the parcellated regions via the conventional LASSO (Fig. 4d). We further showed the DTI-derived white matter fiber bundles connecting to each of six major regions of DMNs in Figs. 4e-4f. We see that the global fiber shape patterns are reasonably consistent between the two subjects for each of the six regions via the structured LASSO (Fig. 4e), while with considerate variability between those via the conventional LASSO (Fig. 4f). Quantitatively, we represented the connection pattern of a fiber bundle as a 144 dimensional vector descriptor (Section 2.3), and defined the connection pattern consistency of two fiber bundles as the Euclidean distance of the two 144 dimensional vectors. The mean fiber connection pattern consistency across the six regions and across any pair of all subjects is 0.46±0.05 via the structured LASSO and 1.55±0.54 via the conventional LASSO. In conclusion, the identified functional networks via the proposed structured LASSO have both reasonable spatial pattern correspondence and fiber connection pattern consistency across subjects compared with those via the conventional LASSO.

3.2 Functional Networks Guided by Multiple Levels of Cortical Parcellation

We further parcellated the cortical surfaces into finer-granularity group-wise consistent patches under the hierarchical scheme detailed in Section 2.3. Another four levels (159, 222, 243, and 250 regions in total based on [6], respectively) besides the first level (Figs. 4a-4b) were obtained and illustrated in Fig. 5. Here we examined the stability and consistency of reconstructed DMNs via the four different levels of cortical parcellation guided structured LASSO in Figs. 5a-5d. The co-visualization of the cortical parcellation with the spatial pattern of identified DMN at each level (the first row of Figs. 5a-5d, respectively) shows that the major regions of DMNs are reasonably matched with specific parcellated regions at each level. Quantitatively, the mean spatial similarity and fiber connection pattern consistency of DMNs across all ten subjects at each level are shown in Fig. 6. In conclusion, the DMNs based on different hierarchical levels of cortical parcellation guided structured LASSO have both higher spatial pattern similarity with the DMN template and fiber connection pattern consistency across subjects compared with those via the conventional LASSO.

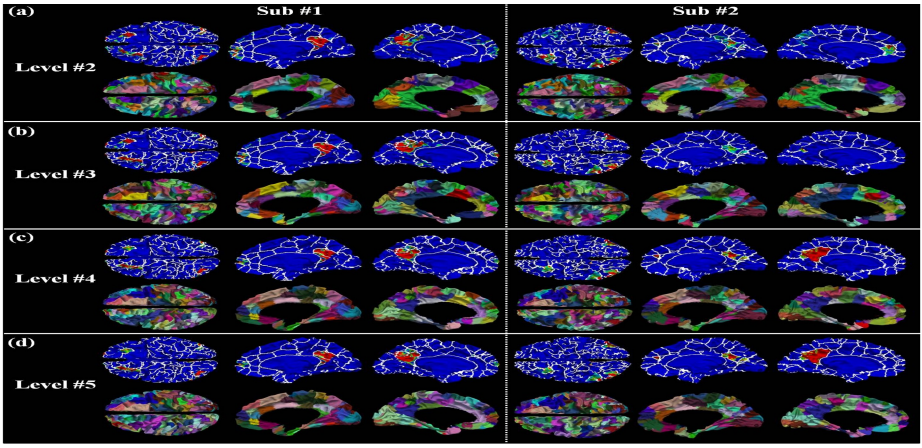

Fig. 5. (a)-(d): Identified DMNs based on another four levels of cortical parcellation guided structured LASSO, respectively. In each sub-figure, the first row shows the co-visualization of the cortical parcellation (white curves delineate the boundaries of regions) and the spatial pattern of DMN, and the second row shows the cortical parcellation at the specific level. The corresponding parcellated regions across subjects are labeled by the same color. Note that there is no correspondence of cortical parcellation color labels across different levels.

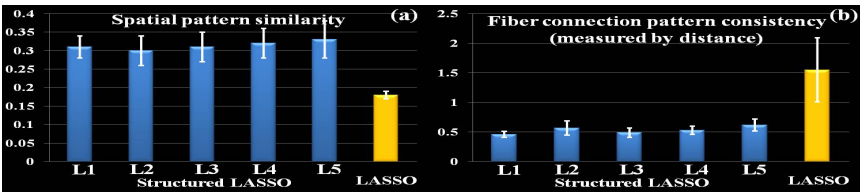

Fig. 6. (a) Mean spatial pattern similarity and (b) fiber connection pattern consistency (defined as the distance in Section 3.1) of DMNs across all ten subjects based on the five levels (indexed by L1 to L5) of cortical parcellation guided structured LASSO and the conventional LASSO.

3.3 Co-visualization of Other Identified Functional Networks

We identified nine functional networks based the network templates in [13]. Note that more networks can be identified if more templates are provided. Fig. 7 co-visualizes the nine functional networks of two example subjects. Specifically, RSNs #1, #2 and #3 are all located at visual cortex. RSNs #4, #5, #6 and #7 are DMN, sensorimotor, auditory, and executive control network, respectively. RSNs #8 and #9 contain middle frontal and superior parietal regions. We see that the major regions of the nine networks have reasonable spatial pattern correspondence and coincidence with specific corresponding parcellated cortical regions across the two example subjects.

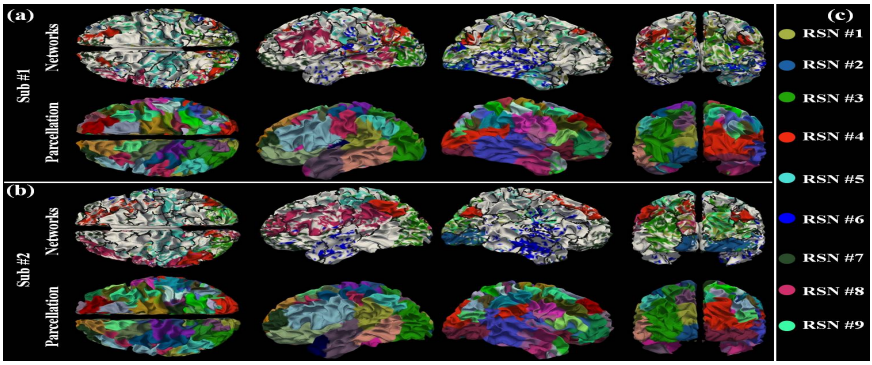

Fig. 7. (a)-(b) Co-visualization of nine functional networks via the structured LASSO of two example subjects. In each sub-figure, the first row co-visualizes the cortical parcellation (black curves delineate the boundaries of regions) and the spatial pattern of nine functional networks. The corresponding functional network is labeled by the same color across subjects as illustrated in (c), and the second row shows the cortical parcellation. The corresponding parcellated regions are labeled by the same color across subjects. Note that there is no correspondence of color labels between functional networks and parcellated regions.

4 Discussion and Conclusion

We proposed a novel fiber connection pattern-guided structured sparse representation of whole-brain rsfMRI signals to infer functionally consistent regions. Experimental

results demonstrated that the identified functional networks achieved both reasonable group-wise spatial pattern correspondence and fiber connection pattern consistency across subjects, which were not well addressed in previous functional atlas. Our future work includes adopting our method to identify network nodes based on the orthogonal dictionary atoms and 'network node hubs' based on the non-orthogonal atoms for conventional functional connectivity network analysis.

Acknowledgements. This research was supported in part by the National Institutes of Health (R01DA033393, R01AG042599), by the National Science Foundation Graduate Research Fellowship (NSF CAREER Award IIS-1149260, CBET-1302089, BCS-1439051), by the Jiangsu Natural Science Foundation (Project No. BK20131351), and by the 111 Project (No.B13022).

References

1. Lee, K., et al.: A data-driven sparse GLM for fMRI analysis using sparse dictionary learning with MDL criterion. IEEE Trans. Med. Imaging 30(5), 1076–1089 (2011)
2. Oikonomou, V.P., et al.: A sparse and spatially constrained generative regression model for fMRI data analysis. IEEE Trans. Biomed. Eng. 59(1), 58–67 (2012)
3. Lv, J., et al.: Holistic atlases of functional networks and interactions reveal reciprocal organizational architecture of cortical function. IEEE Trans. Biomed. Eng. (2014). doi: 10.1109/TBME.2014.2369495
4. Passingham, R.E., et al.: The anatomical basis of functional localization in the cortex. Nat. Rev. Neurosci. 3(8), 606–616 (2002)
5. Venkataraman, A., et al.: Joint modeling of anatomical and functional connectivity for population studies. IEEE Trans. Med. Imaging 31(2), 164–182 (2012)
6. Zhang, T., et al.: Group-wise consistent cortical parcellation based on DTI-derived connectional profiles. In: International Symposium on Biomedical Imaging, pp. 826–829 (2014)
7. Liu J., et al.: Multi-task feature learning via efficient $l_{2,1}$-norm minimization. In: Conference on Uncertainty in Artificial Intelligence, pp. 339–348, arXiv:1205.2631 (2009)
8. Smith, S.M., et al.: Resting-state fMRI in the Human Connectome Project. NeuroImage 80, 144–168 (2013)
9. Sotiropoulos, S.N., et al.: Advances in diffusion MRI acquisition and processing in the Human Connectome Project. Neuroimage 80, 125–143 (2013)
10. Mairal, J., et al.: Online learning for matrix factorization and sparse coding. The Journal of Machine Learning Research 11, 19–60 (2010)
11. Zhu, D., et al.: DICCCOL: dense individualized and common connectivity-based cortical landmarks. Cerebral Cortex 23(4), 786–800 (2013)
12. Tibshirani, R.: Regression shrinkage and selection via the LASSO. Journal of the Royal Statistical Society 58, 267–288 (1996)
13. Smith, S.M., et al.: Correspondence of the brain's functional architecture during activation and rest. Proc. Natl. Acad. Sci. U S A 106(31), 13040–13045 (2009)
14. Jaccard, P.: Étude comparative de la distribution florale dans une portion des Alpes et des Jura. Bulletin de la Société Vaudoise des Sciences Naturelles 37, 547–579 (1901)